August 2003 • NREL/BK-520-34443

13th Workshop on Crystalline Silicon Solar Cell Materials and Processes

Extended Abstracts and Papers

Workshop Chairman/Editor: B.L. Sopori

Program Committee:
J. Rand, T. Saitoh, R. Sinton, M. Stavola,
D. Swanson, T. Tan, E. Weber, J. Werner,
B. Sopori, and M. Al-Jassim

Vail Marriott Mountain Resort
Vail, Colorado
August 10-13, 2003

Prepared under Task No. WO97C100

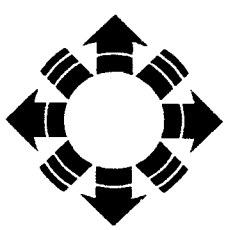

National Renewable Energy Laboratory
1617 Cole Boulevard
Golden, Colorado 80401-3393

NREL is a U.S. Department of Energy Laboratory
Operated by Midwest Research Institute • Battelle • Bechtel

Contract No. DE-AC36-99-GO10337

Statistically meaningful data on the chemical state of iron precipitates in processed multicrystalline silicon using synchrotron-based X-ray absorption spectroscopy

T. Buonassisi[1], M. Heuer[1], A.A. Istratov[1], E.R.Weber[1], Z. Cai[2], B. Lai[2], M. Marcus[3], J. Lu[4], G. Rozgonyi[4], R. Schindler[5], R. Jonczyk[6], and J. Rand[6]

[1]University of California and Lawrence Berkeley National Lab., Berkeley, CA;
[2]Advanced Photon Source, Argonne Nat. Lab., Argonne, IL;
[3]Advanced Light Source, Lawrence Berkeley National Lab., Berkeley, CA;
[4]North Carolina State University, Raleigh, NC;
[5]Fraunhofer Institute for Solar Energy Systems, Freiburg, Germany;
[6]AstroPower Inc., Newark, DE.

X-ray fluorescence microscopy (μ-XRF), x-ray beam induced current (XBIC), and x-ray absorption spectromicroscopy (μ-XAS) were performed on fully-processed BaySix cast multicrystalline silicon and aluminum-gettered AstroPower Silicon-Film™ sheet material. Over ten iron precipitates – predominantly of iron silicide – were identified at low lifetime regions in both materials, both at grain boundaries and intragranular defects identified by XBIC. In addition, large (micron-sized) particles containing oxidized iron and other impurities (Ca, Cr, Mn) were found in BaySix material. The smaller iron silicide precipitates were more numerous and spatially distributed than their larger oxidized iron counterparts, and thus deemed more detrimental to minority carrier diffusion length.

Sample preparation.

Low-lifetime regions of as-grown AstroPower Silicon-Film™ and fully-processed BaySix cast multricystalline material were identified with Electron Beam Induced Current (EBIC) and Laser/Light Beam Induced Current (LBIC), respectively, to determine regions of interest for this study. The AstroPower sample was aluminum gettered at 800°C for 4 hours to simulate actual solar cell gettering. The two materials were then chemically etched to remove the first few microns from the both surfaces, and in the case of the BaySix sample, to remove the anti-reflection coating and frontside metallization grid.

Experimental techniques.

X-ray fluorescence microscopy (μ-XRF) is a powerful technique for mapping the distribution of trace transition metal impurities in silicon.[1,2] The physical principle of μ-XRF is similar to electron microscope-based energy dispersive spectroscopy (EDS), the only difference that synchrotron-based x-rays (and not electrons) are the excitation radiation. As a result, μ-XRF has a much lower Bremsstrahlung background, a larger probing depth that is limited only by the exiting fluorescence attenuation length (36 microns for Fe, 70 microns for Cu), and an overall higher sensitivity compared to its electron counterpart. The only disadvantage is a much larger spot size (50-5000nm) compared with field emission transmission electron microscopes (~0.2nm). Nevertheless, because of the high flux (typically 10^9-10^{11} photons/s) of synchrotron-based XRF systems and a relatively weaker interaction between the excitation radiation and bound electrons, large volumes of material can be probed with high sensitivity, making this an ideal tool for detecting spatially inhomogeneous transition metal precipitates in PV-grade silicon.

In addition, the X-ray Beam Induced Current (XBIC) technique, an x-ray equivalent of Laser/Light Beam Induced Current (LBIC), can yield information about the recombination activity of defects. This powerful combination of XBIC and μ-XRF provides, simultaneously, information about the recombination activity and elemental nature of a transition metal precipitate.

Once an XBIC/μ-XRF map is obtained over a certain area of interest, one can obtain information about the chemical nature of transition metal defects via X-ray Absorption Spectromicroscopy (μ-XAS). μ-XAS is an umbrella term including the X-ray Absorption Near-Edge Spectroscopy (XANES) and Extended X-ray Absorption Fine Structure (EXAFS) techniques. XANES yields information primarily on the oxidation state and immediate environment (first neighbors) of the atoms measured, whereas EXAFS yields information about the extended environment (second, third, etc. neighbors) and bonding configuration of the probed atoms.

For sample pre-characterization, XBIC/μ-XRF were performed on Beamline 10.3.1 of the Advanced Light Source (ALS) of Lawrence Berkeley National Laboratory, with multilayer mirror focusing, optimal peak flux ~10^{10} photons/s, and spot size ~2×2 μm^2. To obtain chemical information from the extended fine structure of select precipitates, XBIC/μ-XRF/μ-XAS were performed on Beamline 10.3.2 of the ALS with multilayer mirror focusing, two-crystal Si (111) constant-exit monochromator, peak flux ~10^{10} photons/s, and minimum spot size ~5x5 μm^2. For detailed mapping and oxidation analysis of smaller precipitates, μ-XRF/XANES were performed at Beamline 2-ID-D of the Advanced Photon Souce (APS) of Argonne National Laboratory with zone plate optics, Kohzu Si (111) monochromator, peak flux ~10^{11} photons/s and spot size ~200x200 nm^2. Although reliable and reproducible XANES could be performed on precipitates equal to or smaller than the beam spot size by eliminating all translational motion of the monochromator crystals and employing a small correction factor for beam defocusing, EXAFS measurements were not possible at 2-ID-D because of current limitations in the focusing optics while scanning over wide energy ranges.

Iron was selected as the choice element of this study, given that it is a proven efficiency killer of silicon devices[3] and is by an order of magnitude the most abundant impurity in mc-Si.[4]

AstroPower results.

The most striking feature of AstroPower material was the extended intragranular iron precipitates (Fig. 1). These precipitates were very noticeable in XBIC, easily located by their strong recombination activity. μ-XANES analyses on these precipitates revealed that iron is present in neutral oxidation state, most likely $FeSi_2$, by comparison with standard material (Fig. 2).

It is possible that these intragranular precipitates are associated with the void/dislocation complexes identified via TEM investigations of *Zhang et al*.[5] The large free surface available at the voids and the strain fields at the associated dislocations offer an abundance of precipitation sites for Fe, and the fact that these complexes are distributed throughout the bulk means that Fe can more quickly diffuse to these structural defects than to other sinks, such as surfaces or grain boundaries.

In addition to these characteristic intragranular defects, a recombination-active grain boundary was scanned with μ-XRF (Fig. 3, scan area 5x35 μm^2) to reveal the fine structure of the Fe precipitates at this extended defect. The grain boundary, the electrical activity of which was characterized by XBIC at ALS Beamline 10.3.1, was located at APS 2-ID-D by the change of intensity of the monochromatic beam scattering peak from one grain to another. In the case of this sample, the variation was high, in the range of 25-27%. This large change in scattering intensities reveals that this is a high angle grain boundary, which previous studies[6] have suggested

should be an efficient sink for metals. Indeed, the μ-XRF analysis revealed a multitude of very small precipitates evenly spaced at the grain boundary. A XANES analysis, shown in Fig. 2, on one such precipitate in Fig. 3 revealed that the precipitate most closely matches $FeSi_2$. Horizontal and vertical μ-XRF scans revealed that the precipitate is smaller than or equal in diameter to the beam spot size of 200nm. By taking a 60 second XRF point scan on the point of maximum signal, and comparing the signal peak intensity with a standard NIST 1833 thin foil, it was possible to obtain a lower estimate the size of the precipitate assuming all Fe is contained in one single spherical $FeSi_2$ precipitate close to the surface by using the following formulae:

$$\text{Fe in Precipitate}\,[\text{atoms/cm}^{-2}] = \frac{\text{Counts/60s/Precipitate}}{\text{Counts/60s/Standard}} \cdot \text{Fe in NIST 1833 Calibration Standard}\,[\text{atoms/cm}^{-2}] \quad (1)$$

$$\text{Volume of Precipitate}\,[\text{cm}^{3}] = \frac{\text{Fe in precipitate}\,[\text{atoms/cm}^{-2}] \cdot \text{Spot Size}\,[\text{cm}^{2}]}{\text{Density of FeSi}_2\,[\text{atoms/cm}^{3}]} \quad (2)$$

Assuming a spherical geometry, the radius of this particular precipitate at the grain boundary was calculated to be 13.8 nm. Notice the denuded zone before the grain boundary contains no such Fe precipitates.

BaySix results.

A particularly recombination-active grain boundary from the bottom of the ingot was characterized by XBIC on ALS Beamline 10.3.1 which revealed a denuded zone. This same area was identified at APS Beamline 2-ID-D via a change in intensity of the elastic scattering peak. It was noted that the change of scattering intensity between grains, while a noticeable 11-12%, was smaller than what was observed in the AstroPower sample, an indication that this might be a smaller angle grain boundary. It is known that "clean" structural defects, especially "gentle" defects such as low-angle grain boundaries, do not tend to have noticeable recombination activity at room temperature.[7] The high recombination activity of this structural defect and the presence of a denuded zone are good indications of the presence of impurities.

A μ-XRF scan located a series of iron-containing precipitates along the length of the grain boundary, as shown in Fig. 4, and summarized in Table 1. Note the step size of the scan shown in Fig. 4 is 3000 nm, while the beam spot size was a mere 200 nm, suggesting even more such precipitates could be present but may have been missed. These precipitates were substantially larger than those noted in AstroPower material (see Table 1). A small 16x16 μm^2 scan was performed along the grain boundary with 200 nm step size, but no precipitates with diameter equal to or less than the spot size were detected within 1s accumulation time, unlike the AstroPower material, indicating that the Fe distribution along the grain boundary of this sample is indeed different.

Table 1. Dimensions and chemical state of the precipitates (* - shown in Fig. 4)

Precipitate Label	X dimension (nm)	Y dimension (nm)	Chemical State
P1	≤200	570	**$FeSi_2$**
P2	~1500	~1200	Fe_2O_3
P3*	1250	892	Fe_2O_3
P4*	275	772	**$FeSi_2$**
P5*	≤200	710	**$FeSi_2$**
P6*	290	547	**$FeSi_2$**

XANES analyses (summarized in Table 1) on the precipitates revealed two general species of iron precipitate: (1) A number of small (≤200-770 nm diameter) precipitates identified as iron silicide ($FeSi_2$). As in the AstroPower sample, these $FeSi_2$ precipitates do not contain other metal impurities. However, the sizes of the precipitates are much larger, and they are distributed with greater distances in between. (2) A few large (>900 nm diameter) oxidized iron clusters, closely resembling the chemical form identified by McHugo et al.[8] While these precipitates contain primarily iron, other impurities (e.g. Cr, Mn, Ca) are also present. It is possible that "large" (on the order of a micron in diameter) pieces of dirt or rusted stainless steel are incorporated into the melt, where at high temperatures, they secrete iron into the surrounding crystal. This iron then precipitates at nearby extended defects, forming $FeSi_2$.

To test this hypothesis, a Czochralski silicon sample with a 1.3 μm polysilicon layer deposited with chemical vapor deposition was contaminated with iron by scratching the backside with a wire. The sample was heated at 1150°C for 2 hours to simulate a high temperature step. The iron gettered to the polysilicon layer was analyzed with μ-XAS at ALS Beamline 10.3.2, yielding an almost perfect match with a $FeSi_2$ standard. This is additional evidence that dissolved iron in multicrystalline silicon tends to precipitate to form iron silicide clusters, which are known to be recombination active lifetime killers.[3] Further investigations must be performed to fully understand this precipitation phenomenon.

Conclusions.

For the first time, statistically meaningful data was acquired on the chemical state of iron precipitates in PV-grade mc-Si. The grand majority of intragranular iron precipitates in AstroPower and iron precipitates at grain bounaries in AstroPower and BaySix materials were identified as iron silicide ($FeSi_2$). Because of the low dissolution barrier of $FeSi_2$ and the numerical abundance of these precipitates, the rate of gettering of iron from these precipitates is thus most likely kinetically-limited as suggested by *Plekhanov et al.*[9], and not dissolution-limited. Nevertheless, at least in BaySix material, a few large impurity precipitates containing primarily oxidized iron but also an abundance of other metals may take much longer to completely dissolve, thus complicating any model of gettering based on a distribution of tiny $FeSi_2$ precipitates.

Acknowledgements.

Special thanks to Elizabeth Schäffer for performing LBIC measurements on BaySix material. This work was funded by NREL subcontract AAT-2-31605-03, and the AG-Solar project of the government of Northrhein-Westfalia (NRW), funded through the Fraunhofer Institute for Solar Energy Systems (ISE) (Germany). The operations of the Advanced Light Source at Lawrence Berkeley National Laboratory are supported by the Director, Office of Science, Office of Basic Energy Sciences, Materials Sciences Division, of the U.S. Department of Energy under Contract No. DE-AC03-76SF00098. Use of the Advanced Photon Source was supported by the U.S. Department of Energy, Office of Science, Office of Basic Energy Sciences, under Contract No. W-31-109-ENG-38.

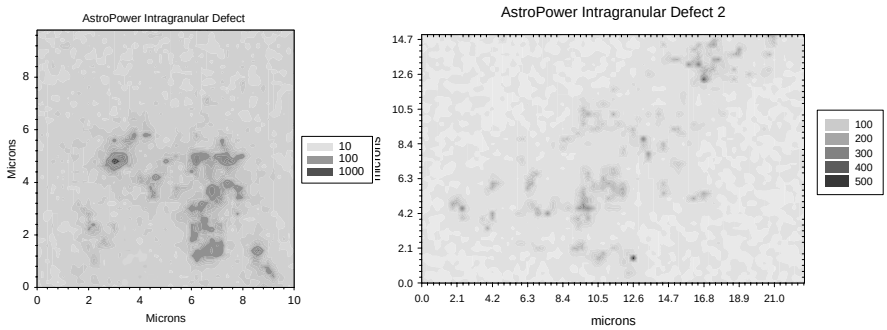

Fig. 1. µ-XRF image of two areas of Astropower material, containing clusters of iron.

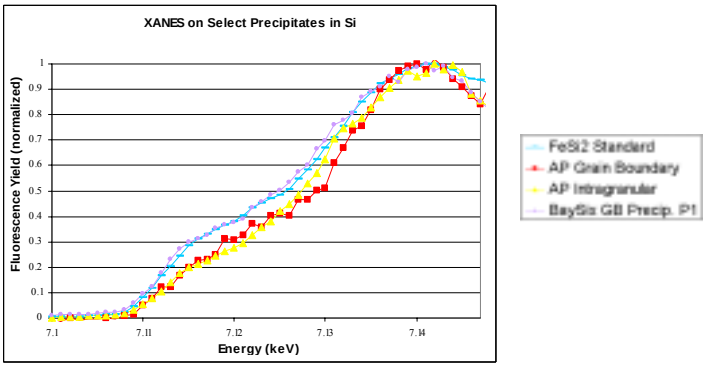

Fig. 2. Comparison of µ-XANES spectra of FeSi2 standard and three iron precipitates found in Astropower (AP) and BaySix materials.

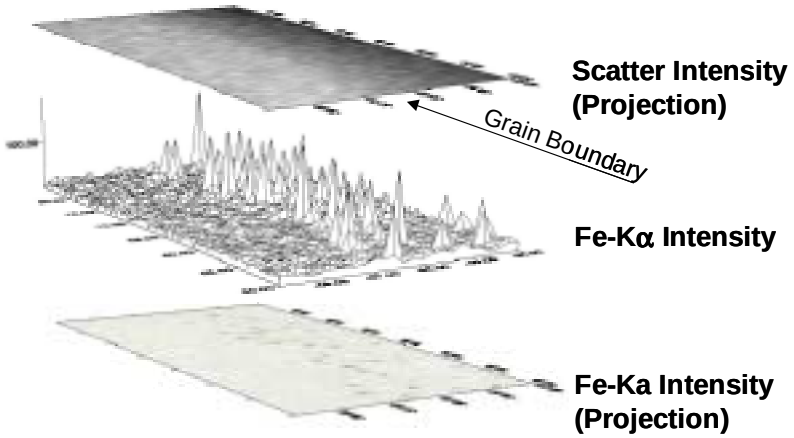

Fig. 3.µ-XRF scan of a grain boundary area of Astropower sample.

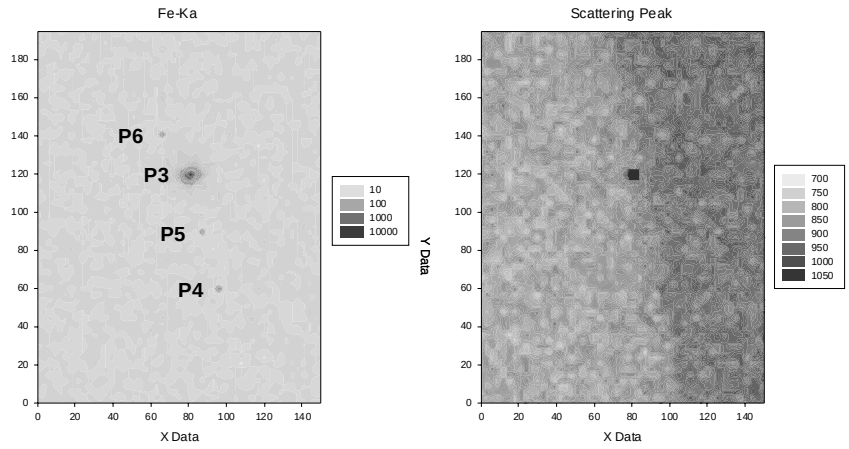

Fig. 4. μ-XRF scan (left) and scattering peak (right) of a grain boundary area of Baysix sample.

REFERENCES.

1 S. A. McHugo, A. C. Thompson, A. Mohammed, G. Lamble, I. Périchaud, S. Martinuzzi, M. Werner, M. Rinio, W. Koch, H.-U. Höfs, and C. Häßler, Journal of Applied Physics **89,** 4282-4288 (2001).

2 S. A. McHugo, A. C. Thompson, C. Flink, E. R. Weber, G. Lamble, B. Gunion, A. Mac-Dowell, R. Celestre, H. A. Padmore, and Z. Hussain, Journal of Crystal Growth **210,** 395-400 (2000).

3 A. A. Istratov, H. Hieslmair, and E. R. Weber, Applied Physics A: Material Science & Processing **70,** 489-534 (2000).

4 A. A. Istratov, T. Buonassisi, E. R. Weber, R. J. McDonald, A. R. Smith, R. Schindler, J. A. Rand, J. Kalejs, *see this volume*.

5 R. Zhang, G. Duscher, J. Rand, and G. A. Rozgonyi, in *Nanoscale investigations of poly-crystalline silicon for photovoltaic applications*, Breckenridge, CO, 2002, p. 206.

6 A. Ihlal, R. Rizk, and O. B. M. Hardouin Duparc, Journal of Applied Physics **80,** 2665-2670 (1996).

7 J. Bailey, and E. R. Weber, Phys. stat. sol. (a) **137,** 515 (1993).

8 S. A. McHugo, A. C. Thompson, G. Lamble, C. Flink, and E. R. Weber, Physica B **273-274,** 371-374 (1999).

9 P. S. Plekhanov, R. Gafiteanu, U. M. Gosele, and T. Y. Tan, Journal of Applied Physics **86,** 2453-2458 (1999).